



Article scientifique

Article

2017

Published version

Open Access

This is the published version of the publication, made available in accordance with the publisher's policy.

---

## Synchrotron Imaging Shows Effect of Ventilator Settings on Intrabreath Cyclic Changes in Pulmonary Blood Volume

---

Porra, Liisa; Broche, Ludovic; Dégrugilliers, Loïc; Albu, Gergely; Malaspinas, Iliona; Doras, Camille; Wallin, Mats; Hallbäck, Magnus; Habre, Walid; Bayat, Sam

### How to cite

PORRA, Liisa et al. Synchrotron Imaging Shows Effect of Ventilator Settings on Intrabreath Cyclic Changes in Pulmonary Blood Volume. In: American Journal of Respiratory Cell and Molecular Biology, 2017, vol. 57, n° 4, p. 459–467. doi: 10.1165/rcmb.2017-0007OC

This publication URL: <https://archive-ouverte.unige.ch/unige:111092>

Publication DOI: [10.1165/rcmb.2017-0007OC](https://doi.org/10.1165/rcmb.2017-0007OC)

# Synchrotron Imaging Shows Effect of Ventilator Settings on Intrabreath Cyclic Changes in Pulmonary Blood Volume

Liisa Porra<sup>1,2</sup>, Ludovic Broche<sup>3</sup>, Loïc Dégrugilliers<sup>4</sup>, Gergely Albu<sup>5</sup>, Iliana Malaspinas<sup>5</sup>, Camille Doras<sup>5</sup>, Mats Wallin<sup>6</sup>, Magnus Hallbäck<sup>6</sup>, Walid Habre<sup>5</sup>, and Sam Bayat<sup>5,7</sup>

<sup>1</sup>Department of Physics, University of Helsinki, Helsinki, Finland; <sup>2</sup>Medical Imaging Center, Helsinki University Hospital, Helsinki, Finland; <sup>3</sup>Hedenstierna Laboratory, Department of Surgical Sciences, Uppsala University, Sweden; <sup>4</sup>Department of Pediatric Intensive Care, Amiens University Hospital, Amiens, France; <sup>5</sup>Anesthesiological Investigations Unit, University Hospitals of Geneva, Geneva, Switzerland; <sup>6</sup>Maquet Critical Care, Solna, Sweden; and <sup>7</sup>University of Grenoble EA-7442 and Department of Clinical Physiology, Sleep and Exercise, Grenoble University Hospital, Grenoble, France

## Abstract

Despite the importance of dynamic changes in the regional distributions of gas and blood during the breathing cycle for lung function in the mechanically ventilated patient, no quantitative data on such cyclic changes are currently available. We used a novel gated synchrotron computed tomography imaging to quantitatively image regional lung gas volume (V<sub>g</sub>), tissue density, and blood volume (V<sub>b</sub>) in six anesthetized, paralyzed, and mechanically ventilated rabbits with normal lungs. Images were repeatedly collected during ventilation and steady-state inhalation of 50% xenon, or iodine infusion. Data were acquired in a dependent and nondependent image level, at zero end-expiratory pressure (ZEEP) and 9 cm H<sub>2</sub>O (positive end-expiratory pressure), and a tidal volume (V<sub>T</sub>) of 6 ml/kg (V<sub>T1</sub>) or 9 ml/kg (V<sub>T2</sub>) at an Inspiratory:Expiratory ratio of 0.5 or 1.7 by applying an end-inspiratory pause. A video showing dynamic decreases in V<sub>b</sub> during inspiration is presented. V<sub>b</sub> decreased with positive end-expiratory pressure ( $P = 0.006$ ;  $P = 0.036$  versus V<sub>T1</sub>-ZEEP and V<sub>T2</sub>-ZEEP, respectively), and showed larger oscillations at the dependent image level, whereas a 45% increase in V<sub>T</sub> did not have a significant effect. End-inspiratory V<sub>b</sub> minima were reduced by an end-inspiratory pause ( $P = 0.042$ ,  $P = 0.006$  at nondependent and dependent levels, respectively). Normalized

regional V<sub>g</sub>:V<sub>b</sub> ratio increased upon inspiration. Our data demonstrate, for the first time, within-tidal cyclic variations in regional pulmonary V<sub>b</sub>. The quantitative matching of regional V<sub>g</sub> and V<sub>b</sub> improved upon inspiration under ZEEP. Further study is underway to determine whether these phenomena affect intratidal gas exchange.

**Keywords:** mechanical ventilation; ventilation distribution; synchrotrons; perfusion imaging; X-ray computed tomography

## Clinical Relevance

Our data demonstrate, for the first time, cyclic variations in regional pulmonary blood volume (V<sub>b</sub>) during the respiratory cycle. The magnitude of the cyclic changes in regional V<sub>b</sub> was significantly affected by gravity, positive end-expiratory pressure, and Inspiratory:Expiratory ratio. The quantitative matching of regional gas volume and V<sub>b</sub> improved upon inspiration under zero end-expiratory pressure. Further study is underway to determine whether these phenomena affect intra-tidal gas exchange.

Changes in lung volume during positive-pressure ventilation have a significant effect on pulmonary vascular resistance (PVR) in normal lung. Pulmonary blood vessels

act as Starling resistors, differentially affected by their surrounding pressure as well as by radial interstitial tethering forces determined by lung volume (1).

Under mechanical ventilation, the rise in lung volume above functional residual capacity (FRC) during inspiration causes the transmural pressure in small pulmonary

(Received in original form January 9, 2017; accepted in final form May 9, 2017)

This work was supported by the European Synchrotron Radiation Facility and Swiss National Science Foundation grant 332003B-143331/1, and by the Tampere Tuberculosis Foundation Finland (L.P.).

Author Contributions: L.P., L.B., G.A., M.W., M.H., and S.B. designed the study; L.P., L.B., L.D., G.A., I.M., C.D., M.W., M.H., W.H., and S.B. acquired, analyzed, or interpreted data; G.A. and S.B. drafted the manuscript; all authors critically revised the manuscript before submission.

Correspondence and requests for reprints should be addressed to Sam Bayat, M.D., Ph.D., Department of Clinical Physiology, Sleep, and Exercise, Grenoble University Hospital, Boulevard de la Chantourne, 38700 La Tronche, France. E-mail: sbayat@chu-grenoble.fr

This article has an online supplement, which is accessible from this issue's table of contents at [www.atsjournals.org](http://www.atsjournals.org)

The uncompressed videos are accessible from this article's supplementary material page.

Am J Respir Cell Mol Biol Vol 57, Iss 4, pp 459–467, Oct 2017

Copyright © 2017 by the American Thoracic Society

Originally Published in Press as DOI: 10.1165/rcmb.2017-0007OC on May 23, 2017

Internet address: [www.atsjournals.org](http://www.atsjournals.org)

arterioles, capillaries, and veinules—referred to as alveolar vessels—to drop, reducing their volume and increasing resistance to flow (2). Larger pulmonary arteries and veins categorized as extra-alveolar vessels are more affected by radial interstitial tethering forces that increase their volume upon inspiration. The overall effect of lung inflation above FRC is a reduced pulmonary blood volume (Vb) that raises the lung vascular resistance and right ventricular afterload (2). On the other hand, the intrathoracic pressure increases during positive-pressure breathing directly affect right atrial pressure, causing venous return to decrease. This, in turn, may reduce right ventricular filling and stroke volume, an important determinant of pulmonary Vb (3).

Most of what is known on the interaction between lung volume, alveolar pressure ( $P_{alv}$ ), and the pulmonary capillary volume and calibers is based on studies in static conditions, either of the relation between airway pressures and PVR (4, 5), or postmortem capillary morphology (6, 7). The oscillations in pulmonary Vb are, however, likely to occur dynamically within the respiratory cycle. These oscillations have been indirectly estimated by comparing right and left ventricular outflows in pigs (8).

Despite the potential significance of dynamic changes in the regional distributions of gas and blood during the breathing cycle for lung function in the mechanically ventilated patient, no quantitative data on such cyclic changes are currently available. Importantly, there are little if any data on the effect of mechanical ventilation settings, such as tidal volume ( $V_T$ ) and positive end-expiratory pressure (PEEP) on dynamic changes in Vb distribution with assisted breathing.

Here, we describe an imaging technique that allows mapping the dynamic changes in the regional distribution of blood and gas volumes (Vg) within the respiratory cycle, under mechanical ventilation. The technique uses dual energy synchrotron radiation beams to image the quantitative distribution of contrast elements, such as inhaled stable xenon (Xe) gas within the airspaces, or injected iodine in blood (9, 10). We introduced a gating procedure through which the regional distributions of gas and blood could be mapped at several time points during the respiratory cycle. The present study was undertaken to test the

**Table 1.** Arterial Blood Gases

	Arterial Blood Gases		
	Vt1-ZEEP	Vt2-ZEEP	Vt1-PEEP
PaO <sub>2</sub> , mm Hg	262.5 ± 11.1	277.8 ± 8.5	270.2 ± 3.2
PaCO <sub>2</sub> , mm Hg	38.7 ± 2.3	39.4 ± 4.0	42.8 ± 2.8
pH	7.42 ± 0.02	7.37 ± 0.03	7.34 ± 0.03
HCO <sub>3</sub> <sup>-</sup> , mmol/L	25.1 ± 2.3	22.1 ± 2.1	22.7 ± 2.4

*Definition of abbreviations:* HCO<sub>3</sub><sup>-</sup>, arterial bicarbonate concentration; PaCO<sub>2</sub>, arterial carbon dioxide pressure; PaO<sub>2</sub>, arterial oxygen pressure; PEEP, positive end-expiratory pressure; Vt, tidal volume; ZEEP, zero end-expiratory pressure.

Data are mean ± SE. There were no significant differences in any of the parameters between the experimental conditions.

hypothesis that regional blood distribution within the lung varies dynamically during the breathing cycle. We further assessed the effect of gravity,  $V_T$ , end-expiratory pressure, and the inclusion of an inspiratory pause, on the dynamic changes in regional blood and gas distributions. Some of the results of these studies have been previously reported in the form of an abstract (11).

## Materials and Methods

### Animal Preparation

A detailed description of the experimental procedures is provided in the online supplement. The experiments were performed on six upright rabbits (2.9 ± 0.1 kg), anesthetized, paralyzed, and

mechanically ventilated in volume-control mode, initially with: a  $V_T$  of 6 ml/kg; a fraction of inspired oxygen of 0.5; an inspiratory:expiratory (I:E) ratio of 1:2; a PEEP of 3 cm H<sub>2</sub>O; and a respiratory rate set to obtain an arterial carbon dioxide pressure of approximately 40 mm Hg. The animals were immobilized in an upright position for imaging.

### Study Protocol

After a recruitment maneuver (20 cm H<sub>2</sub>O, 10 s), ventilation settings were randomly assigned to either 0 PEEP (ZEEP) and a  $V_T$  of 6 ml/kg (Vt1-ZEEP), ZEEP and a  $V_T$  of 9 ml/kg (Vt2-ZEEP), or PEEP of 9 cm H<sub>2</sub>O and Vt1 (Vt1-PEEP). Synchrotron imaging was performed consecutively at a dependent and nondependent axial image level, during Xe

**Table 2.** Hemodynamic Parameters

	Systemic Hemodynamic Parameters		
	Vt1-ZEEP	Vt2-ZEEP	Vt1-PEEP
PaS, mm Hg			
No EIP	94.2 ± 7.7	105.2 ± 4.7	97.1 ± 6.4
EIP	90.7 ± 7.7*	101.2 ± 5.1*	92.6 ± 6.5*
PaM, mm Hg			
No EIP	82.1 ± 5.8	92.7 ± 3.3	87.3 ± 5.6
EIP	78.8 ± 5.7*	88.0 ± 3.8*	83.5 ± 5.7*
PaD, mm Hg			
No EIP	76.0 ± 5.0	86.5 ± 2.9	82.4 ± 5.2
EIP	72.8 ± 4.7*	81.4 ± 3.5*	78.9 ± 5.4*
ΔPaS, mm Hg			
No EIP	4.9 ± 0.5	7.4 ± 1.5	5.8 ± 1.7
EIP	12.5 ± 1.4*	17.5 ± 3.4*	14.3 ± 3.9*

*Definition of abbreviations:* ΔPaS, change in systolic pressure during the respiratory cycle; EIP, end-expiratory pause; PaD, diastolic arterial pressure; PaM, mean arterial pressure; PaS, systolic arterial pressure; PEEP, positive end-expiratory pressure; Vt, tidal volume; ZEEP, zero end-expiratory pressure.

Data are mean ± SE. There were no significant differences between experimental conditions. PaS, PaM, and PaD are averaged over the entire respiratory cycle

\* $P < 0.05$  EIP versus no EIP.

inhalation (50% in O<sub>2</sub>) with each ventilation setting, in random order. Imaging was repeated after iodine contrast injection (10 ml iomeprol). To assess the effect of a sustained versus transient inflation on within-breath changes in V<sub>b</sub>, a 1.2-second end-inspiratory pause (EIP) was included in every other respiratory cycle, increasing I:E from 0.5 to 1.7.

### Synchrotron Radiation Computed Tomography Imaging

The experiments were performed at the European Synchrotron Radiation Facility (ESRF-ID17, Grenoble, France). K-edge subtraction (KES) imaging allows quantitative measurements of regional specific ventilation, V<sub>g</sub>, and V<sub>b</sub> (10, 12). The methodology has been described previously (9, 12–14). Briefly, this imaging technique uses two X-ray beams at slightly different energies that can be tuned above and below the K-shell energy (34.56 keV) of a contrast element, such as Xe or iodine. Two computed tomography images are thus simultaneously acquired during the inhalation of stable Xe or infusion of iodine. The density due to the contrast element can be separated from that of tissue in each image voxel using a specifically developed computer algorithm (9, 10, 13, 15).

### Image Gating Procedure and Analysis

Cross-sectional images can be reconstructed from 720 line projections acquired over 360° in 1 second. We used a gating procedure where projections were acquired continuously over 200 seconds during continuous ventilation (see Figure E1 in the online supplement). A sequence of two respiratory cycles, one of which included an EIP, was divided into 30 consecutive intervals. By sorting the projections belonging to a specific within-breath interval and projection angle from the entire acquisition, we were able to reconstruct two-dimensional cross-sectional images at each of the 30 time intervals. Regional V<sub>g</sub>s and V<sub>b</sub>s were summed within each axial image level and expressed versus time.

### Statistical Analysis

The scatters in the parameters were expressed by the SEM values. Two-way repeated measures ANOVA was applied with ventilation setting and pattern (EIP versus no EIP) or level (nondependent versus dependent) as within-subject variables. Blood gas data were analyzed

**Table 3.** Airway Pressures and Tidal Volumes

	Airway Pressures and V <sub>T</sub> s		
	V <sub>T</sub> 1-ZEEP	V <sub>T</sub> 2-ZEEP	V <sub>T</sub> 1-PEEP
V <sub>T</sub> , ml	19.5 ± 1.3	28.3 ± 1.8*	19.6 ± 1.3 <sup>†</sup>
P <sub>max</sub> , cmH <sub>2</sub> O	21.1 ± 1.5	30.3 ± 2.3*	31.2 ± 1.0*
P <sub>plat</sub> , cmH <sub>2</sub> O	16.6 ± 1.6	24.4 ± 2.6*	27.5 ± 1.0* <sup>†</sup>
PEEP, cmH <sub>2</sub> O	0.8 ± 0.3	0.8 ± 0.5	9.4 ± 0.3* <sup>†</sup>

*Definition of abbreviations:* PEEP, positive end-expiratory pressure; P<sub>max</sub>, peak airway pressure; P<sub>plat</sub>, plateau pressure; V<sub>T</sub>, tidal volume; ZEEP, zero end-expiratory pressure.

Data are mean ± SE.

\*P < 0.05 versus V<sub>T</sub>1-ZEEP.

<sup>†</sup>P < 0.05 versus V<sub>T</sub>2-ZEEP.

by one-way repeated-measures ANOVA. Pairwise comparisons were performed by using Student-Newman-Keuls multiple comparison procedures. Comparison of regional V<sub>b</sub> between standard and gated KES images was performed by paired Student's *t* test. The statistical analyses were conducted using SigmaPlot (version 11.0; Systat Software, Inc., Chicago, IL). All statistical tests were performed with a significance level of *P* less than 0.05.

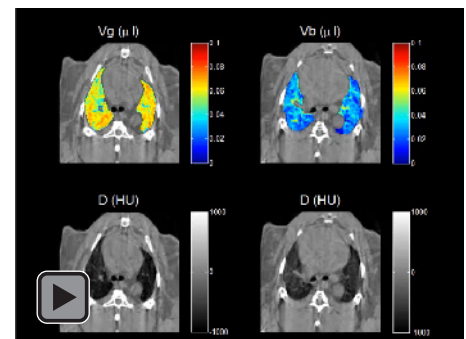
## Results

Gas exchange data are summarized in Table 1. There were no significant differences in the arterial blood gases between the ventilation settings. The systemic hemodynamic data are shown in Table 2. There was no significant difference in systolic and mean arterial pressures (P<sub>pas</sub>) between ventilation settings. In respiratory cycles with an EIP, P<sub>pas</sub> were lower, and the drop in systolic pressure during the respiratory cycle was larger regardless of the ventilation settings (*P* = 0.002, *P* < 0.001, and *P* < 0.001 in V<sub>T</sub>1-ZEEP, V<sub>T</sub>2-ZEEP, and V<sub>T</sub>1-PEEP, respectively). V<sub>T</sub>, maximal and plateau pressure, and PEEP are summarized in Table 3. Plateau pressure was lowest on V<sub>T</sub>1-ZEEP followed by V<sub>T</sub>2-ZEEP (*P* < 0.001 versus V<sub>T</sub>1-ZEEP), and highest on V<sub>T</sub>1-PEEP (*P* < 0.001 versus V<sub>T</sub>2-ZEEP).

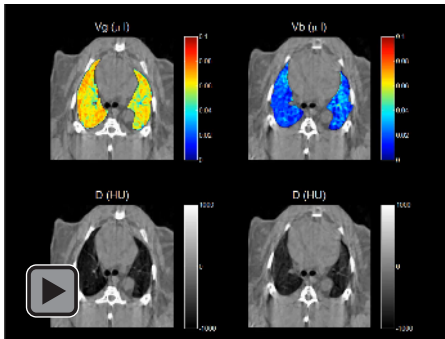
Video animations showing the within-breath changes in regional lung gas and blood distributions were produced with each ventilation setting. Representative examples at V<sub>T</sub>1-ZEEP are included in the online supplement (Videos 1 and 2). Simultaneous images showing lung tissue density were obtained and are included. The latter demonstrated no sign of cyclic recruitment

of atelectasis. In addition, both Xe and tissue-density projection images showed no evidence of atelectasis (Figure E2). Figure 1 shows still images of the regional gas and blood distributions at both axial levels, at end-expiration and end-inspiration at V<sub>T</sub>1-ZEEP. Similar images in the other experimental settings can be found in the online supplement (Figure E3). Comparison of standard KES images at iodine energy obtained on V<sub>T</sub>1-ZEEP during a single end-expiratory apnea with gated end-expiratory images (*n* = 6 animals × two levels) showed no significant difference in regional V<sub>b</sub> (*P* = 0.119).

Upon inspiration, as regional V<sub>g</sub> increased, V<sub>b</sub> decreased, with the opposite occurring during expiration. Cyclic variations of both parameters with time are shown in Figures 2 and 3. Although the absolute value of regional gas was larger at the dependent level, the relative changes in V<sub>g</sub> were similar at the two image levels. In addition, V<sub>b</sub> was consistently lower in the ventral compared with the dorsal half of



**Video 1.** Representative video animation showing the within-tidal evolution of regional gas (V<sub>g</sub>; left column) and blood (V<sub>b</sub>; right column) distribution in the nondependent image slice in the V<sub>T</sub>1-ZEEP condition. Lower row shows corresponding tissue density images. V<sub>T</sub>, tidal volume; ZEEP, zero end-expiratory pressure.



**Video 2.** Representative video animation showing the within-tidal evolution of regional gas ( $V_g$ ; left column) and blood ( $V_b$ ; right column) distribution in the nondependent image slice in the  $V_{T2}$ -ZEEP condition. Lower row shows corresponding tissue density images.

the image slice, although intrabreath oscillations were not significantly affected by anatomic location within the image slice (Figure E5, Table E1). Conversely, the intrabreath oscillations in regional  $V_b$  were larger at the dependent compared with the nondependent level (Figure 3). These oscillations were significantly affected by PEEP: the end-expiratory maxima in regional  $V_b$  (Figure 4) were significantly lower on PEEP compared with both ZEEP conditions ( $P = 0.006$ ,  $P = 0.036$  versus  $V_{T1}$ -ZEEP and  $V_{T2}$ -ZEEP, respectively). In addition, the magnitude of  $V_b$  oscillation was reduced by PEEP at the dependent image level.  $V_T$ , however, did not significantly affect the end-expiratory maximal values of  $V_b$  ( $P = 0.139$ ,  $V_{T2}$ -ZEEP

versus  $V_{T1}$ -ZEEP). On the other hand, the effect of PEEP and  $V_T$  on the minimum  $V_b$ s at end inspiration was not statistically significant. The end-inspiratory minima were slightly, but significantly, reduced during the EIP at both axial image levels ( $P = 0.042$ ,  $P = 0.006$  at nondependent and dependent levels, respectively) compared with the breath without an EIP.

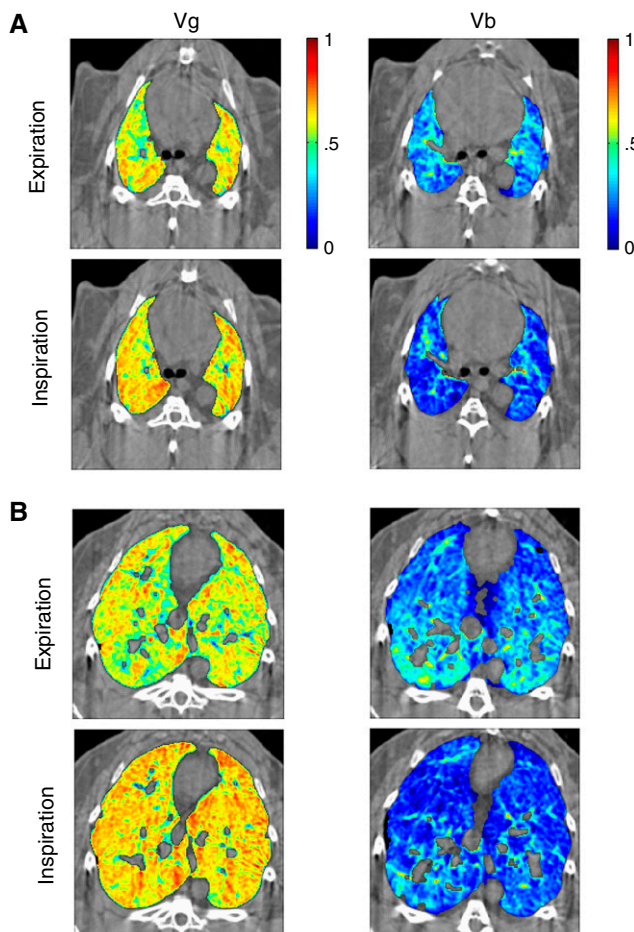
The inhomogeneity in gas distribution, as reflected by the SD of Xe concentration, decreased significantly upon inspiration (Figure E4) at both image levels, on  $V_{T1}$ -ZEEP and  $V_{T2}$ -ZEEP. On  $V_{T1}$ -PEEP, at end-expiration, the SD values were significantly lower than  $V_{T1}$ -ZEEP, without significant within-tidal changes thereafter. The inhomogeneity in blood distribution also significantly decreased, but only at the dependent level under  $V_{T1}$ -ZEEP conditions (Figure E5).

Figure 5 shows the relationship between regional  $V_g$  and  $V_b$ s at the two axial image levels. At both levels, dynamic intrabreath changes in regional  $V_b$  depended on the amount of gas, regardless of  $V_T$  and PEEP. Although significant at both levels, this relationship was stronger at the dependent level.

The time evolution of the ratio of mean-normalized  $V_g$  to  $V_b$  is shown in Figure 6. This parameter rose upon inspiration and dropped during expiration. The end-expiratory minima were significantly increased by PEEP ( $P = 0.004$ ,  $P = 0.010$  versus  $V_{T1}$ -ZEEP and  $V_{T2}$ -ZEEP, respectively at the nondependent level, and  $P < 0.001$  versus both  $V_{T1}$ -ZEEP and  $V_{T2}$ -ZEEP at the dependent level). The end-inspiratory maximal values were above 1 and approached roughly 1.2, particularly at the nondependent level (Figure 7), and were slightly, but significantly, higher during the EIP ( $P = 0.001$ ,  $P < 0.001$  at the nondependent and dependent levels, respectively). Cardiac output (CO) measured in a separate group of supine animals is shown in Figure E7. This parameter did not change significantly at higher  $V_T$ , but was reduced with PEEP.

## Discussion

The goal of this study was to describe how regional lung  $V_b$  dynamically changes within the breathing cycle under mechanical ventilation, and to determine the effect of gravity,  $V_T$ , PEEP, and an increased I:E



**Figure 1.** Representative composite image frames showing the regional distribution of gas (gas volume [ $V_g$ ]; left column) and blood (blood volume [ $V_b$ ]; right column) within nondependent (A) and dependent (B) lung regions, at end-expiration (top rows) and end-inspiration (bottom rows), in a representative animal at tidal volume ( $V_T$ ) 1-zero end-expiratory pressure. Corresponding videos showing the dynamic changes within the respiratory cycle at both image levels in all experimental conditions are included (Videos 1–6).

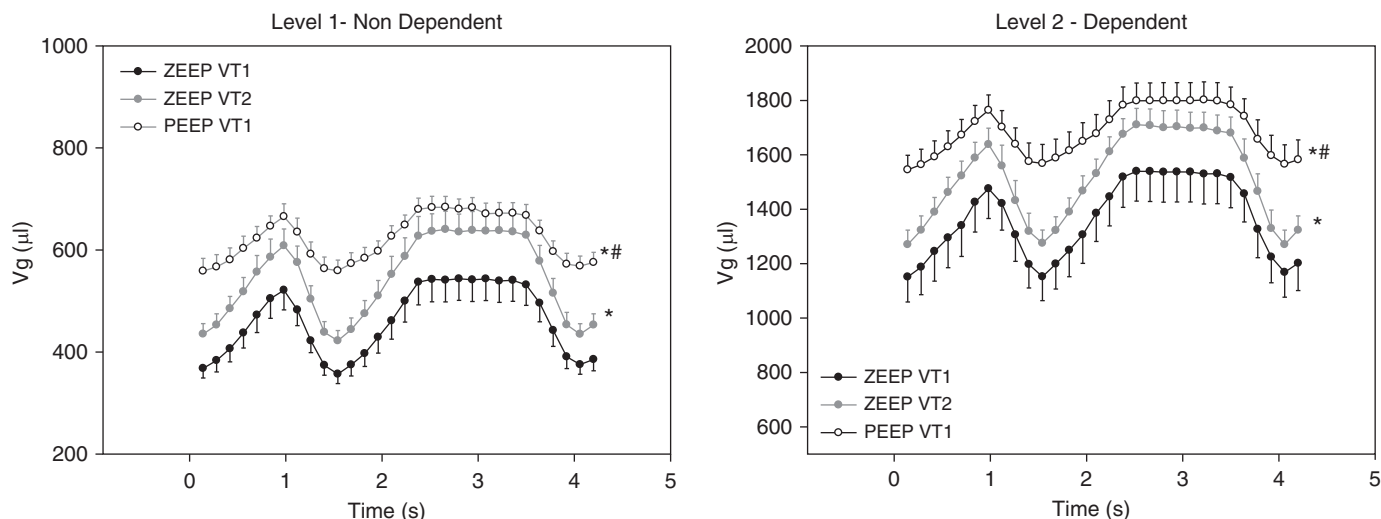


**Figure 2.** Time evolution of the mean regional lung Vg in the nondependent and dependent image slices during two successive respiratory cycles with and without an end-inspiratory pause. Data are mean ( $\pm$ SE) ( $n = 6$ ). \* $P < 0.05$  versus Vt1 zero end-expiratory pressure (ZEEP); # $P < 0.05$  versus Vt2 ZEEP. PEEP, positive end-expiratory pressure; Vt, tidal volume.

ratio on this distribution. To our knowledge, this is the first time the dynamic changes of regional Vb are described *in vivo* in an intact lung. Our data show that: (1) regional Vb cyclically decreases with lung inflation; (2) the magnitude of this decrease was larger at the dependent image level; (3) a 45% increase in VT did not have a significant effect, whereas a PEEP of 9 cmH<sub>2</sub>O decreased the regional Vb; and (4) increasing I:E through an end-inspiratory pause caused further dynamic decreases in regional Vb.

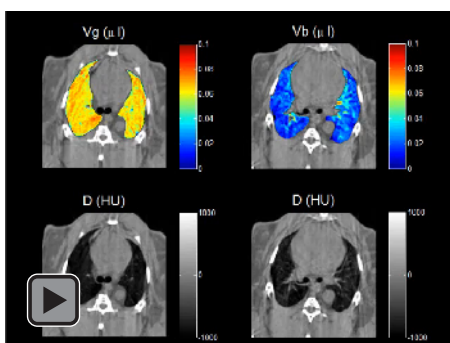
Upon inspiration, the increase in the gas fraction within the image voxels leads to an apparent dilution of blood and tissue. Using KES imaging, blood and

tissue are measured separately, assuming all iodine contrast is contained in the blood. Moreover, upon inspiration, the volume of lung tissue within the image slice increases, whereas the fraction of blood within each image voxel decreases. If the apparent dilution of blood by air, previously referred to as the “Slinky effect” (16), were the only mechanism at play, then summing up the Vb contained in each image voxel over the entire image slice should not show any significant variation between inspiration and expiration. Conversely, we found that the sum of the blood content of all voxels within the lung image decreases on inspiration, despite a larger number of voxels. The decrease in regional Vb upon inspiration could, therefore, not be explained merely by lung tissue deformation.

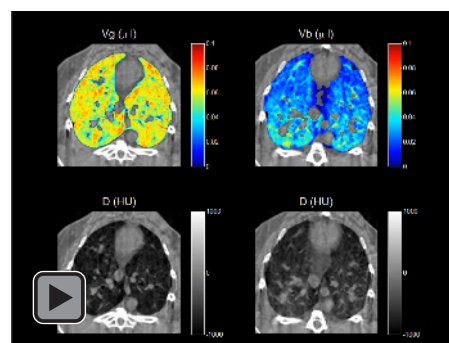
Mechanisms potentially involved in the cyclic variations of regional Vb under positive-pressure ventilation are multiple. First, the increase in intrathoracic pressure and lung volume during assisted inspiration reduces systemic venous return and right ventricular preload, due to the concomitant rise in right atrial pressure (17). Both increases in VT and PEEP can contribute to this mechanism (18).

Second, positive P<sub>alv</sub> during inspiration can reduce the volume of alveolar vessels. Because of the initial work of Permutt, Howell, and colleagues (1), pulmonary vasculature is considered to comprise two different categories of blood vessels: those in the immediate vicinity of the alveolar

septa, which are subject to intra-alveolar pressure, and the so-called extra-alveolar vessels, which are dependent on the interstitial pressure. The latter are influenced by the radial interstitial tethering forces, and see their volumes increase as lung volume is raised above FRC (19). These two compartments are oppositely affected by lung inflation. Lung volume and the relative values of P<sub>alv</sub>, P<sub>pa</sub>, and venous pressure (P<sub>pv</sub>) to each other are known to affect alveolar capillary dimensions (20). Part of the current understanding of this relationship is based on morphometric data (7, 21, 22). Mazzone (7), in rapidly frozen dog lung, showed that alveolar capillary dimensions show a remarkable decrease under zone 2 conditions



**Video 3.** Representative video animation showing the within-tidal evolution of regional gas (Vg; left column) and blood (Vb; right column) distribution in the nondependent image slice in the Vt1-PEEP condition. Lower row shows corresponding tissue density images.



**Video 4.** Representative video animation showing the within-tidal evolution of regional gas (Vg; left column) and blood (Vb; right column) distribution in the dependent image slice in the Vt1-ZEEP condition. Lower row shows corresponding tissue density images.

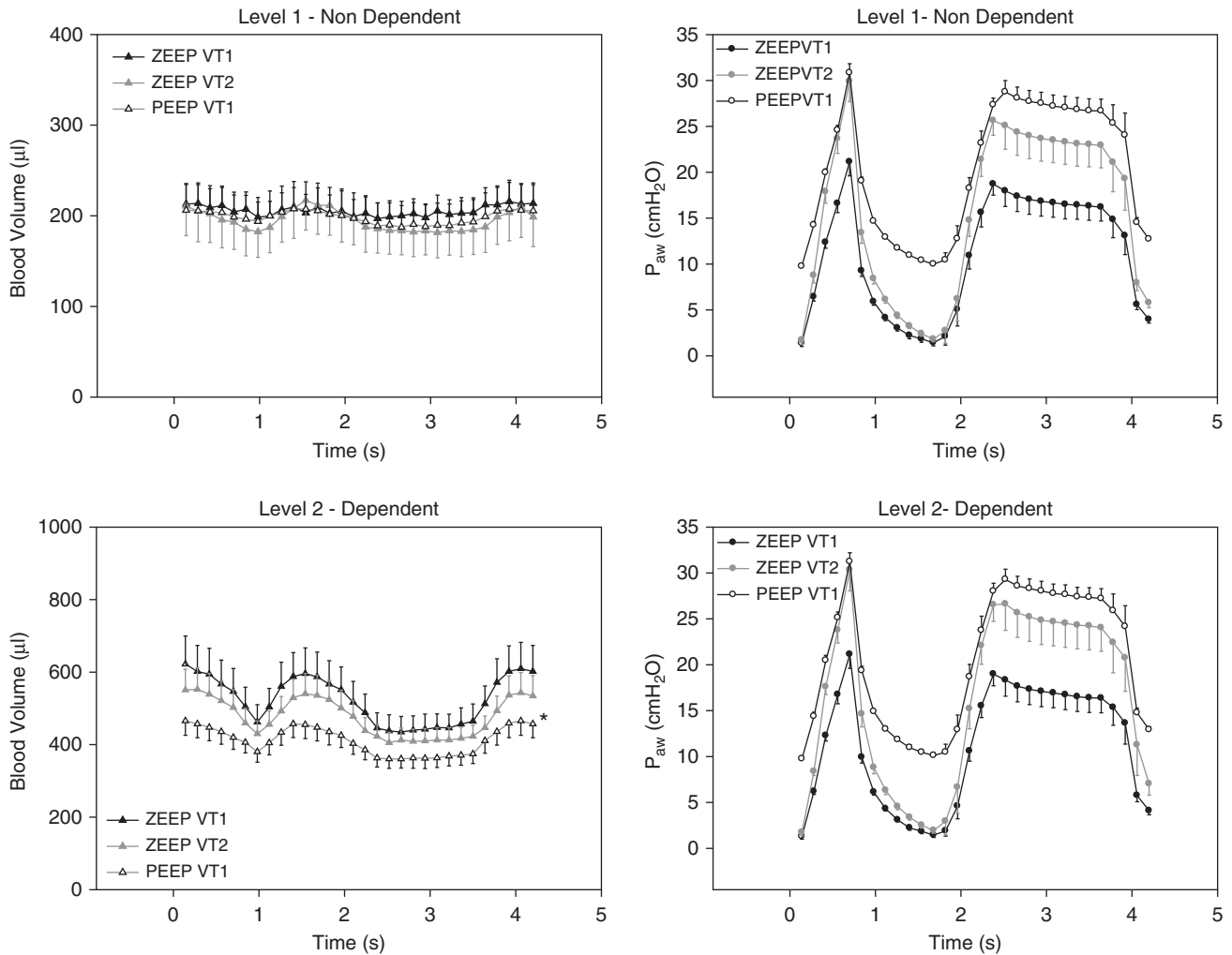


**Figure 3.** Time evolution of the mean regional lung Vb in the nondependent and dependent image slices during two successive respiratory cycles with and without an end-inspiratory pause. Data are mean ( $\pm$ SE) ( $n=6$ ). \* $P < 0.05$  versus Vr1-(ZEEP).

( $P_{pa} > P_{alv} > P_{pv}$ ) as  $P_{alv}$  is increased from 5 to 25 cmH<sub>2</sub>O. The magnitude of this drop was highly dependent on the gravitational changes in capillary pressure, and was almost completely blunted at the less dependent part of zone 2. Our finding, that the dynamic decreases in regional Vb during inspiration were more pronounced in the dependent lung slice, which was on average 20 mm caudal to the nondependent image slice, is in agreement with these morphometric data. This phenomenon is further illustrated by the sharper slope of the regional Vb versus Vg relationship in the more dependent lung image (Figure 5), whereas the changes in Vg were more similar between the two image levels. In this study, larger extra-alveolar vessels were excluded from the Vb maps; however, small, subresolution extra-alveolar vessels

( $\leq 0.5$  mm) could not be eliminated, and therefore contribute to the average regional changes in Vb, which therefore represents a net effect. Together, our data suggest that the cyclic changes in Vb distribution result from the interaction between lung volume and the relative values of alveolar luminal and intravascular pressures. These cyclic variations are not uniform throughout the lung, and depend on gravimetric changes in transcapillary pressure.

The decrease in alveolar capillary caliber and volume during positive-pressure inspiration translates into an increase in PVR and right ventricular afterload. Beck and Lai-Fook (23) previously showed in *in situ*-isolated rabbit lung that perfusion decreases as lung volume is increased under zone 3 ( $P_{pv} > P_{alv}$ ) conditions, with an even

larger relative decrease under zone 2. Dawson and colleagues (5), in isolated, perfused cat lung, found that lung capillary resistance increases as the lung is inflated, and that it represents the larger portion of the total PVR at the higher lung volumes. The increase in PVR with lung inflation contributes to the reduction in CO. Here again, both PEEP and high VTs can contribute to this mechanism. We found that a moderate PEEP of 9 cmH<sub>2</sub>O decreased both the mean Vb (Figure 3) and its maximal expiratory value (Figure 4). In the additional group of animals, in which CO was measured by thermodilution (which can be seen as a mean value over the whole respiratory cycle), the same level of PEEP decreased CO, whereas a higher VT of 9 ml/kg did not. The lack of a significant effect of VT may have been due to the

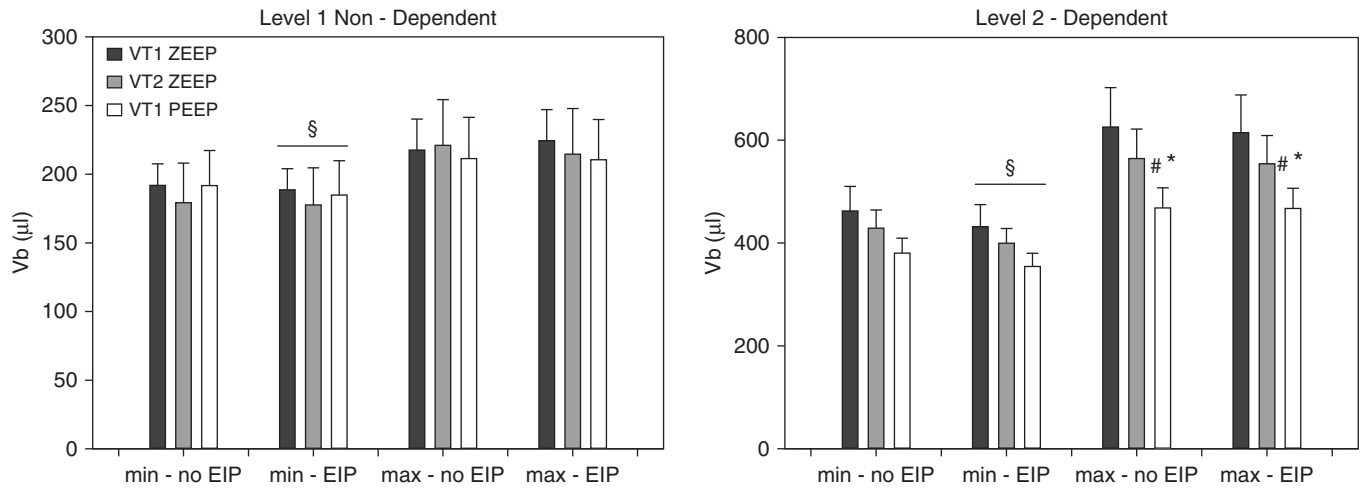


**Figure 4.** Maximal (end-expiratory) and minimal (end-inspiratory) mean regional Vb; EIP, end-inspiratory pause. \* $P < 0.05$  versus Vr1 zero end-expiratory pressure (ZEEP); # $P < 0.05$  versus Vr2-ZEEP; § $P < 0.05$  versus no EIP.

moderate increase of 45%, and larger increases may have produced a more significant change. Alternatively, a potential drop in CO upon inspiration under higher VT values may be compensated during expiration, whereas this is not the case on PEEP. Moreover, the variation in pulmonary Vb also depends on the volemic status, which was stably maintained in this study. On the other hand, an increase in I:E from 0.5 to 1.7 through an EIP slightly, but significantly, decreased the minimal regional Vb, regardless of PEEP or VT. This difference was also seen in the systemic hemodynamic parameters, where mean P<sub>pa</sub> was slightly lower and the inspiratory-to-expiratory drop in systolic pressure was

larger during EIP. This suggests that the decrease in regional pulmonary Vb during positive-pressure inflation, presumably through the compression and progressive emptying of intra-alveolar microvasculature (8), is a time-dependent phenomenon.

The ratio of normalized regional Vg to Vb ( $V_{g_n}/V_{b_n}$ , Figure 6) showed that this parameter increased during inspiration, reaching almost 1.0 at VT1-ZEEP, at both axial image levels, whereas it decreased cyclically to approximately 0.6 on expiration. Therefore, in baseline conditions, the quantitative correspondence between  $V_{g_n}$  and  $V_{b_n}$  improved during inspiration. This could have a potential effect on within-breath gas exchange, but

we cannot confirm this finding based on the present data. Further study is needed to investigate this hypothesis through concomitant rapid measurements of arterial carbon dioxide pressure in normal and pathologic lung, particularly in models of acute respiratory distress syndrome, where the current imaging methodology can help elucidate the impact of ventilation settings on regional lung function (24).

With a PEEP of 9 cmH<sub>2</sub>O, the  $V_{g_n}:V_{b_n}$  ratio exceeded 1.0 at both axial image levels. The same effect on the  $V_{g_n}:V_{b_n}$  ratio was observed with the higher VT, but only at the nondependent image level. A possible explanation is the similar relative increase in  $V_{g_n}$  at the nondependent as compared

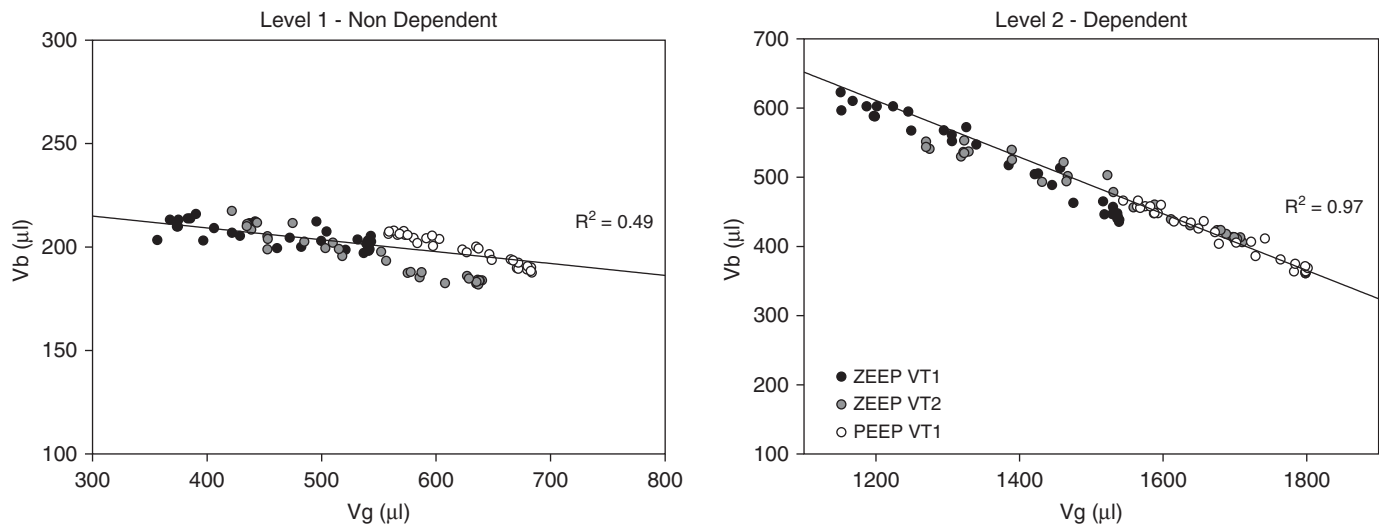


**Figure 5.** Inverse correlation between mean regional Vb and Vg during the respiratory cycle. Data are means over the entire image slice at each time point and condition.

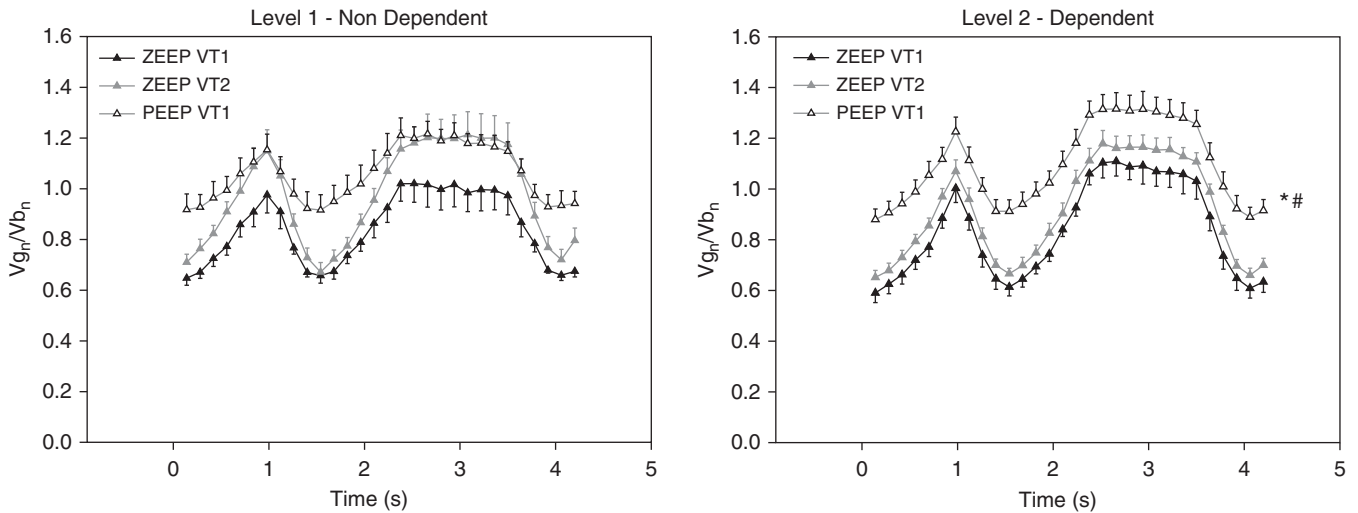


**Figure 6.** Time evolution of the normalized (*n*)  $Vg_n:Vb_n$  ratio in the nondependent and dependent image slices during two successive respiratory cycles with and without an end-inspiratory pause. Data are mean ( $\pm$ SE) ( $n=6$ ). \* $P < 0.05$  versus  $Vt_1$ -(ZEEP); # $P < 0.05$  versus  $Vt_2$ -(ZEEP).

with the dependent level, whereas the drop in  $Vb$  was smaller in magnitude in the nondependent image slice, both under PEEP and the higher  $V_T$ . The higher  $Vg_n:Vb_n$  ratios approaching 1.2 suggest a possible dead-space effect at end inspiration under these conditions, which could negatively impact gas exchange.

**Study Limitations**

Our study had several limitations. Pulmonary  $P_{pa}$  and flow could not be measured, due to the technical complexity of the setup. These would have been helpful in further characterizing the impact of the regional changes in  $Vb$  distribution on PVR. The number of experimental

conditions that could be tested was limited to two axial image levels, one higher  $V_T$  and one level of PEEP, due to time-limited access to the imaging facility. Ideally, a larger range of each parameter should have been tested, which was not possible, due to time-limited access to the imaging facility. In addition, the imaging technique does not yet allow dynamically imaging the lung in three dimensions, although an ongoing upgrade in the imaging setup may allow the acquisition of volumetric data in the near future. Although the major airways and blood vessels were removed by segmentation before analysis, vessels the diameters of which were less than approximately 1.5 mm could not be

excluded. These vessels may include small arteries, arterioles, and small veins. The majority of studies on the partition of blood within the pulmonary vasculature in dog and man indicate that the bulk of pulmonary  $Vb$  is contained in the capillaries (25–27). Finally, the lung was imaged in the vertical position. This was dictated by the geometry of the imaging setup, where the fan beam is horizontally oriented. This means that there is no gravitational gradient within the depicted images. Alike many previous studies in the isolated perfused lung model in the literature, this position allowed us to assess the effect of gravity on the regional cyclic changes in  $Vb$ .

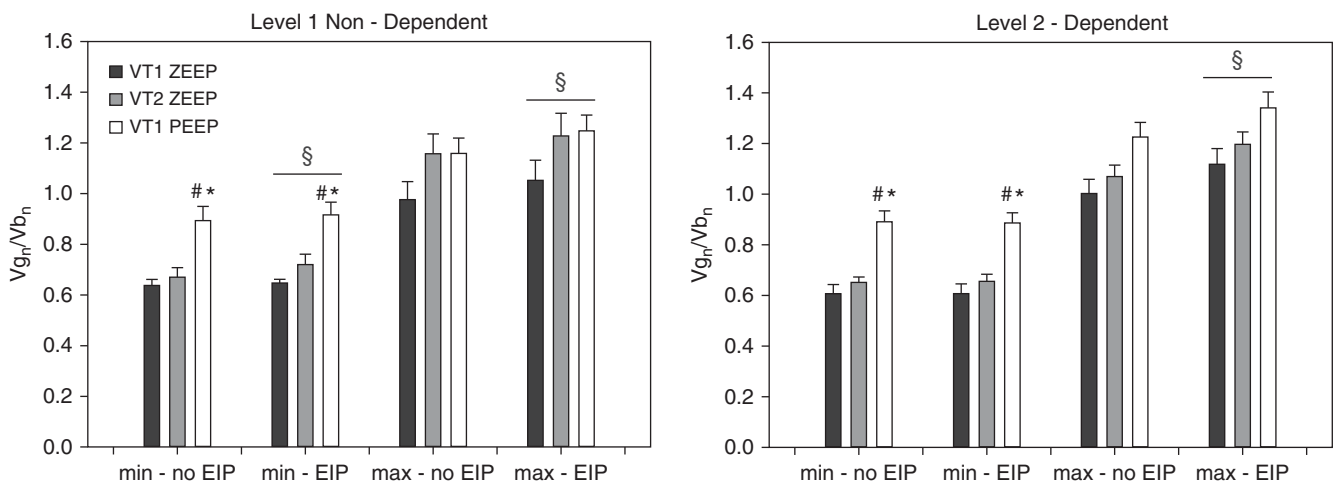
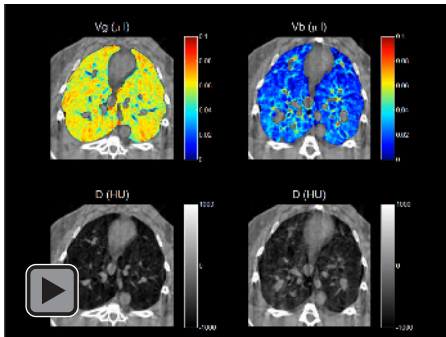


**Figure 7.** Maximal (end-inspiratory) and minimal (end-expiratory) mean normalized  $Vg_n:Vb_n$  ratio. \* $P < 0.05$  versus  $Vt_1$ -(ZEEP); # $P < 0.05$  versus  $Vt_2$ -(ZEEP); § $P < 0.05$  versus no EIP.



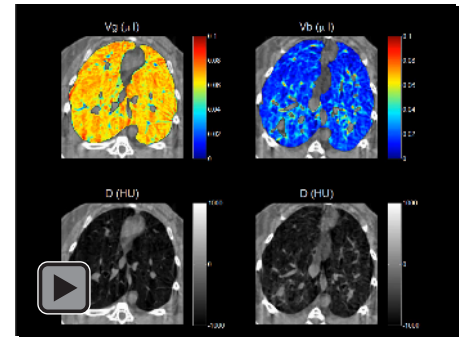
**Video 5.** Representative video animation showing the within-tidal evolution of regional gas (Vg; left column) and blood (Vb; right column) distribution in the dependent image slice in the  $V_T2$ -ZEEP condition. Lower row shows corresponding tissue density images.

## Conclusions

We used a synchrotron computed tomography imaging technique that allows mapping the dynamic changes in the

regional distribution of Vb and Vg within the respiratory cycle in anesthetized, paralyzed, and mechanically ventilated rabbit with normal lungs. Our data demonstrate, for the first time, cyclic variations in regional pulmonary Vb over the course of the respiratory cycle. The magnitude of the cyclic changes in regional Vb was larger in the dependent region of the lung, and both the average value and cyclic variations in regional Vb were decreased by a PEEP of 9 cmH<sub>2</sub>O. Increasing the I:E ratio from 0.5 to 1.7 also reduced the regional Vb during inspiration, whereas the effect of a 45% increase in  $V_T$  was not significant. The quantitative matching of regional Vg and Vb improved upon inspiration under ZEEP. Further study will determine whether these phenomena affect intratidal gas exchange. ■

**Author disclosures** are available with the text of this article at [www.atsjournals.org](http://www.atsjournals.org).



**Video 6.** Representative video animation showing the within-tidal evolution of regional gas (Vg; left column) and blood (Vb; right column) distribution in the dependent image slice in the  $V_T1$ -PEEP condition. Lower row shows corresponding tissue density images.

**Acknowledgments:** The authors thank Christian Nemoz and Herwig Requardt of the European Synchrotron Radiation Facility, Grenoble, France for technical assistance.

## References

- Howell J, Permutt S, Proctor D, Riley R. Effect of inflation of the lung on different parts of pulmonary vascular bed. *J Appl Physiol* 1961;16:71–76.
- Mitzner W, Chang H. Hemodynamics of the pulmonary circulation. In: Scharf SM, Cassidy SS, editors. Heart-lung interactions in health and disease. Vol. 42. New York: Taylor & Francis; 1989. pp. 561–631.
- Pinsky MR. Cardiovascular issues in respiratory care. *Chest* 2005;128:592S–597S.
- West JB, Dollery CT, Naimark A. Distribution of blood flow in isolated lung; relation to vascular and alveolar pressures. *J Appl Physiol* 1964;19:713–724.
- Dawson CA, Grimm DJ, Linehan JH. Effects of lung inflation on longitudinal distribution of pulmonary vascular resistance. *J Appl Physiol* 1977;43:1089–1092.
- Glazier JB, Hughes JM, Maloney JE, West JB. Measurements of capillary dimensions and blood volume in rapidly frozen lungs. *J Appl Physiol* 1969;26:65–76.
- Mazzone RW. Influence of vascular and transpulmonary pressures on the functional morphology of the pulmonary microcirculation. *Microvasc Res* 1980;20:295–306.
- Versprille A, Jansen JR. Tidal variation of pulmonary blood flow and blood volume in piglets during mechanical ventilation during hyper-, normo- and hypovolaemia. *Pflügers Arch* 1993;424:255–265.
- Bayat S, Le Duc G, Porra L, Berruyer G, Nemoz C, Monfraix S, Fiedler S, Thomlinson W, Suortti P, Standertskjold-Nordenstam CG, et al. Quantitative functional lung imaging with synchrotron radiation using inhaled xenon as contrast agent. *Phys Med Biol* 2001;46:3287–3299.
- Suhonen H, Porra L, Bayat S, Sovijärvi AR, Suortti P. Simultaneous *in vivo* synchrotron radiation computed tomography of regional ventilation and blood volume in rabbit lung using combined K-edge and temporal subtraction. *Phys Med Biol* 2008;53:775–791.
- Porra L, Wallin M, Hallbäck M, Broche L, Suortti P, Sovijärvi A, Petak F, Habre W, Bayat S. Changes in regional distribution of gas and blood volumes within a single respiratory cycle: effect of tidal volume, PEEP and respiratory pattern [abstract]. *Eur Respir J* 2014;44:543.
- Monfraix S, Bayat S, Porra L, Berruyer G, Nemoz C, Thomlinson W, Suortti P, Sovijärvi AR. Quantitative measurement of regional lung gas volume by synchrotron radiation computed tomography. *Phys Med Biol* 2005;50:1–11.
- Bayat S, Stregell S, Porra L, Janosi TZ, Petak F, Suhonen H, Suortti P, Hantos Z, Sovijärvi AR, Habre W. Methacholine and ovalbumin challenges assessed by forced oscillations and synchrotron lung imaging. *Am J Respir Crit Care Med* 2009;180:296–303.
- Porra L, Monfraix S, Berruyer G, Le Duc G, Nemoz C, Thomlinson W, Suortti P, Sovijärvi AR, Bayat S. Effect of tidal volume on distribution of ventilation assessed by synchrotron radiation CT in rabbit. *J Appl Physiol* 2004;96:1899–1908.
- Elleaume H, Charvet AM, Corde S, Esteve F, Le Bas JF. Performance of computed tomography for contrast agent concentration measurements with monochromatic X-ray beams: comparison of K-edge versus temporal subtraction. *Phys Med Biol* 2002;47:3369–3385.
- Hopkins SR, Henderson AC, Levin DL, Yamada K, Arai T, Buxton RB, Prisk GK. Vertical gradients in regional lung density and perfusion in the supine human lung: the Slinky effect. *J Appl Physiol* 1985;2007:240–248.
- Pinsky M. Effects of mechanical ventilation on heart-lung interactions. In: Hill NS, Levy MM, editors. Ventilator management strategies for critical care. New York: Taylor & Francis; 2001. pp. 655–692.
- Michard F, Teboul J-L. Using heart-lung interactions to assess fluid responsiveness during mechanical ventilation. *Crit Care* 2000;4:1.
- Lopez-Muniz R, Stephens N, Bromberger-Barnea B, Permutt S, Riley R. Critical closure of pulmonary vessels analyzed in terms of Starling resistor model. *J Appl Physiol* 1968;24:625–635.
- Townsley MI. Structure and composition of pulmonary arteries, capillaries, and veins. *Compr Physiol* 2012;2:675–709.
- Ciurea JS, Gil J. Morphometry of capillaries in three zones of rabbit lungs fixed by vascular perfusion. *Anat Rec* 1996;244:182–192.
- Weibel ER, Untersee P, Gil J, Zulauf M. Morphometric estimation of pulmonary diffusion capacity. VI. Effect of varying positive pressure inflation of air spaces. *Respir Physiol* 1973;18:285–308.
- Beck KC, Lai-Fook SJ. Pulmonary blood flow vs. gas volume at various perfusion pressures in rabbit lung. *J Appl Physiol (1985)* 1985;58:2004–2010.
- Porra L, Bayat S, Malaspinas I, Albu G, Doras C, Broche L, Stregell S, Petak F, Habre W. Pressure-regulated volume control vs. volume control ventilation in healthy and injured rabbit lung: an experimental study. *Eur J Anaesthesiol* 2016;33:767–775.
- Brody JS, Stemmler EJ, DuBois AB. Longitudinal distribution of vascular resistance in the pulmonary arteries, capillaries, and veins. *J Clin Invest* 1968;47:783–799.
- Milnor WR, Jose AD, McGaff CJ. Pulmonary vascular volume, resistance, and compliance in man. *Circulation* 1960;22:130–137.
- Dawson CA, Linehan JH, Rickaby DA. Pulmonary microcirculatory hemodynamics. *Ann N Y Acad Sci* 1982;384:90–106.